

Lawsonite-bearing eclogite from a tectonic mélange in the Ligurian Alps: new constraints for the subduction plate-interface evolution

MARCO SCARSI*, CRISTINA MALATESTA & SILVIA FORNASARO

DISTAV, University of Genova, Genova, Italy

(Received 11 October 2016; accepted 3 April 2017; first published online 23 May 2017)

Abstract – Lawsonite eclogites are rare rocks and have been described from only a few localities in the world. Lawsonite-bearing assemblages are highly unstable and physico-chemical processes linked to exhumation may destroy them; only aggregates interpreted as pseudomorphs after lawsonite could be often recognized. In this paper, we present a detailed structural and petrological study of an area in the northwestern sector of the metaophiolitic high-pressure Voltri Massif (Ligurian Western Alps, Italy). The study area is characterized by a lawsonite-bearing eclogitic metagabbro associated with carbonated serpentinites and glaucophanic metasediments. The metagabbro body reached eclogitic metamorphic peak conditions at $T = 465\text{--}477\text{ }^{\circ}\text{C}$ and $P = 20.9\text{--}24.4\text{ kbar}$, with H_2O continuously supplied to the system. H_2O under-saturated conditions, with the occurrence of both lawsonite and epidote, characterized the exhumation path. Both the low temperature recorded by the body and the occurrence of variously carbonated serpentinites led us to interpret this area as a portion of the top of the subducted slab, coupled with a ‘cool’ mantle wedge, where both aqueous fluids and carbonate-rich fluids were present. The occurrence of rocks belonging to different paleogeographic domains (e.g. continent versus ocean) and the multiple deformations recorded by the metagabbro suggest that this area was nearby the slab–mantle interface. This sector was thus affected by a shear regime that acted in a low-viscosity serpentinite channel, bringing these high-pressure rocks back to the surface.

Keywords: lawsonite-bearing eclogite, subduction plate interface, low-viscosity serpentinite channel, Ligurian Western Alps, Voltri Massif

1. Introduction

Lawsonite blueschists and eclogites are expected to be the prevailing lithotypes developing during deep subduction of the oceanic crust and should therefore be quite abundant in exhumed subduction complexes (Ravna *et al.* 2010). Thermal and chemical models predict that lawsonite should be widespread in subducted oceanic crust at pressure higher than 1.5 GPa (Zack *et al.* 2004). Nevertheless, lawsonite-bearing eclogites have been described from only a few localities in the world (e.g. McBirney, Aoki & Bass, 1967; Watson & Morton, 1969; Krogh, 1982; Caron & Péquignot, 1986; Lardeaux *et al.* 1986; Oh, Liou & Maruyama, 1991; Ghent, Stout & Erdmer, 1993; Shibakusa & Maekawa, 1997; Parkinson *et al.* 1998; Carswell *et al.* 2003; Och *et al.* 2003; Usui *et al.* 2003; Altherr *et al.* 2004; Harlow *et al.* 2004; Mattinson *et al.* 2004; Tsujimori, Liou & Coleman, 2005; Tsujimori *et al.* 2006a,b; Davis & Whitney, 2006; Usui, Nakamura & Helmstaed, 2006; Zhang & Meng, 2006; Zhang, Meng & Wan, 2007; Ghent, Tinkhan & Marr, 2009; Ravna *et al.* 2010; Tsujimori & Ernst, 2014; Vitale Brovarone & Beyssac, 2014). When formed, lawsonite-bearing assemblages are observed to be highly unstable and

their preservation requires to be accompanied by substantial cooling and a rapid uplift (Compagnoni & Maffeo, 1973; Carswell, 1990; Poli & Schmidt, 1995; Maruyama *et al.* 1997; Okamoto & Maruyama, 1999; Forneris & Holloway, 2004; Zack *et al.* 2004; Zhang & Meng, 2006; Brun & Faccenna, 2008; Agard *et al.* 2009; Ravna *et al.* 2010; López-Carmona *et al.* 2011; Zucali & Spalla, 2011). Overprinting by heating and fluid infiltration can destroy mineral assemblages typical of blueschist- and eclogite-facies conditions; as a result these assemblages are rare, and those preserving lawsonite-bearing eclogites are the rarest of all (Davis & Whitney, 2006).

In this paper we present the structural and petrological study of a lawsonite-bearing eclogitic metagabbro, cropping out in the north-western sector of the metaophiolitic Voltri Massif (Ligurian Western Alps, Italy).

The main metagabbro body is a 20 m sized lens, in contact with Na-amphibole-bearing metasediments; both are interlayered with serpentinite schists. The area is characterized also by the occurrence of ophicalcites and serpentinites with a variable degree of carbonation, up to their complete transformation into listvenites. The latter are the result of hydrothermal metasomatic processes related to intense CO_2 -rich fluid circulation (Hansen *et al.* 2005).

* Author for correspondence: marco.scarsi@edu.unige.it

In the last few years both the occurrence of high-pressure C-bearing lithologies and the mechanisms of interaction of CO₂-rich fluids with rocks have been extensively examined to evaluate the carbon fluxes in subduction zones and the turnover rate of CO₂ to the atmosphere (e.g. Kerrick & Connolly, 1998; Ague & Nicolescu, 2014; Kelemen & Manning, 2015).

The aim of this paper is dual: (i) to study the structural and petrological features of the lawsonite-bearing eclogitic metagabbro, to infer its *P–T*-Deformation history, and (ii) to derive further information on the tectono-metamorphic history of the area, i.e. to understand the tectonic evolution at a subduction plate interface (Cannaò *et al.* 2016).

2. Geological background

The Voltri Massif is located at the southernmost termination of the Western Alps (Fig. 1a) and it is made up of metaophiolitic rocks associated with metasediments and slices of subcontinental lithospheric mantle. These rocks underwent a complex Alpine tectono-metamorphic evolution, with blueschist- to eclogite-facies peak metamorphism with variable retrogressive overprints (Chiesa *et al.* 1975; Capponi, 1987, 1991; Capponi *et al.* 1994; L. Crispini, unpub. Ph.D. thesis, Univ. degli Studi di Genova, 1996; Capponi & Crispini, 2002, 2008b).

The Voltri Massif metaophiolites largely consist of serpentinites with metagabbros and lenses of metabasite; metasediments represent the cover of the ophiolitic basement and encompass the whole range from quartzschist to calcschist and micaschist, and are locally associated with metabasites (Chiesa *et al.* 1975; Cortesogno & Forcella, 1978). In the study area, slices of continent-derived metasediment (i.e. quartzites and marbles) and subcontinental mantle (i.e. lherzolites, harzburgites with minor pyroxenites and dunite bodies) occur. Outcrops of upper Eocene – lower Miocene sedimentary deposits of the Tertiary Piedmontese Basin (TPB) cover the Voltri Massif rocks in nonconformity.

In general, the main lithologies of the Voltri Massif show several superposed structures, achieved under different tectonic conditions and ranging from ductile to brittle regime (Capponi & Crispini, 2002). The oldest structures are eclogite/blueschist-facies foliation and rootless hinges of isoclinal folds that lack continuity across outcrops; they are related to subduction events. Later D₁/D₂ similar folds form under Na-amphibole greenschist to greenschist *sensu stricto* metamorphic conditions; overprinting of D₂ on the D₁ folds caused type 3 and rarely type 2 (Ramsay & Huber, 1987) interference patterns. The D₁ and D₂ schistosity produce a composite fabric (CF), which is the most evident surface on the field and controls the contacts between different lithologies.

Ductile structures recording extension parallel to the foliation (i.e. shear bands, boudins, foliation boudinage and extensional veins; Capponi & Crispini, 1997) developed under greenschist-facies conditions.

A detailed description of the main structural features and evolution of the Voltri Massif can be found in Capponi (1987, 1991), Capponi *et al.* (1994), L. Crispini (unpub. Ph.D. thesis, Univ. degli Studi di Genova, 1996) and Capponi & Crispini (2002, 2008b).

3. Geology of the studied area

The study area is located along the Roboaro River (GPS coordinates N44.544686°, E8.436038°), near Sassello village. This area is part of the metaophiolitic Voltri Massif and is characterized by the occurrence of rocks with different paleogeographic origins (oceanic versus continental). The main lithologies are, in decreasing order of areal extent, serpentinite, metagabbro, metabasite lenses (15 to 20 m wide) and ophi-carbonate (Fig. 1b), derived from the ancient ocean-floor of the Ligurian Tethys; restricted outcrops of both ocean- (i.e. glaucophane-bearing calcschists) and continent-derived metasediments (i.e. dolostone) are present in the area; TPB sedimentary deposits widely occur.

We focused on an eclogitic metagabbro lens wrapped by serpentinites and glaucophanic metasediments. The serpentinites are antigorite-bearing with a mylonitic texture characterized by a pervasive foliation that dips NE–NW (Fig. 1b). They are affected by a variable degree of carbonation, propagating in mesh fractures (Fig. 2a) or in fractures parallel to the schistosity; locally serpentinites are completely transformed into listvenite.

The glaucophane-bearing metasediments are commonly associated with the metagabbro lenses (Fig. 2b); they include syn-kinematic stable calcite + dolomite + white mica + chlorite + Na-amphibole + titanite (replacing rutile) + quartz + opaque minerals (e.g. pyrite) and rare apatite; relict intrafoliar folds develop a pervasive axial plane schistosity moderately dipping to the NE–NW (Fig. 3).

The main schistosity in both the serpentinite and metasediment is a composite foliation, related to the superposition of synmetamorphic deformational events.

The metagabbro lens shows a peculiar alternation of Na-amphibole-rich blue layers and Ca–Na-pyroxene-rich green layers, with a mylonitic texture (Fig. 4). Both layers include isoclinal intrafoliar folds (D₁) that are the oldest recognizable event. D₁ folds develop a pervasive Na-amphibole-bearing axial plane schistosity. The metagabbro was affected by a following folding event (D₂), testified to by isoclinal folds (Figs 2c, 3), deforming all the previous structures and causing the alternation of the green and blue bands; the superposition of D₁ and D₂ structures produced a composite fabric dipping NE–NW, which shows the same attitude of the surrounding serpentinite and metasediment schistosity. Extension of fold limbs caused a millimetre- to centimetre-scale dominant symmetric boudinage of the ‘rigid’ Ca–Na-pyroxene-rich green layers (Figs 2d, 4) and the development of low-angle

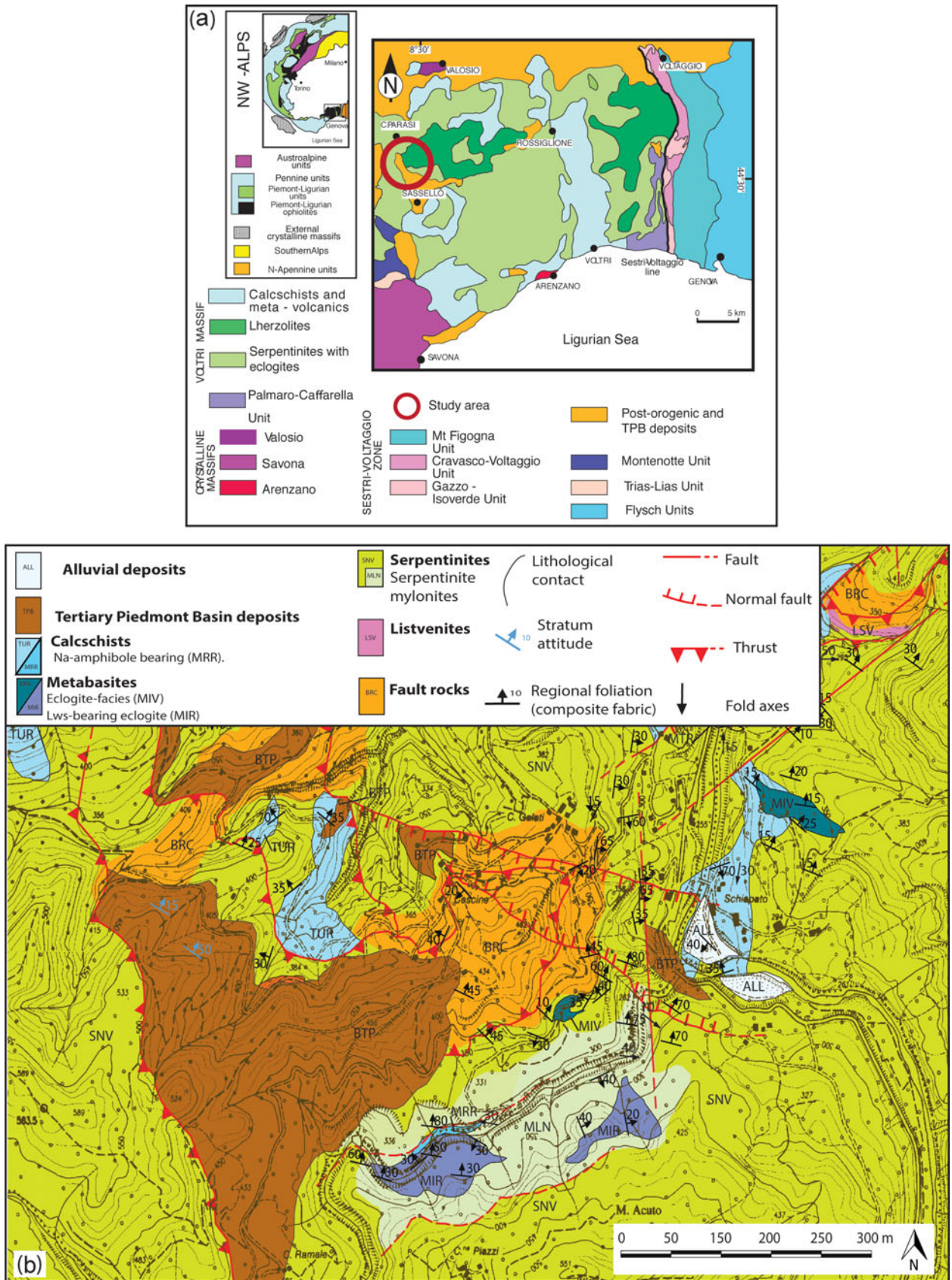


Figure 1. (Colour online) (a) Structural sketch map of the eastern Ligurian Alps and adjoining units; in the top left inset a structural sketch map of the Western Alps is shown. (b) Geological map of the studied area surrounding the Roboaro River.



Figure 2. (Colour online) (a) Brecciated and carbonated serpentinites. (b) Overview of the metagabbro body and the glaucophanic metasediment lens. (c) Isoclinal fold (D_2) inside the metagabbro body deforming a Na-amphibole-rich blue layer. (d) Detail of the layering in the metagabbro body and boudinage of the Ca–Na-pyroxene-rich green layer. Pen for scale is 15 cm long; coin is 2.5 cm diameter.

shearing surfaces, defining an asymmetric boudinage, in the ‘soft’ Na-amphibole-rich blue layers. Indeed, the centimetre-thick Ca–Na-pyroxene-rich layers show prevailing straight to locally oblique necks, in which albite + titanite + Fe-oxide grow along the direction of maximum extension.

The TPB outcrops are at the top of the meta-ophiolitic sequence and show a sub-horizontal bedding.

The study area is also characterized by two main fault-systems: one is represented by high-angle to sub-vertical normal faults, whereas the other system is represented by a low-angle thrust fault, with splays isolating sigmoidal bodies.

4. Petrography of the lawsonite-bearing eclogitic metagabbro

The alternating green and blue layers, defining the composite fabric of the metagabbro body, are Ca–Na-pyroxene and Na-amphibole-rich respectively.

The green layers include millimetre- to centimetre-sized porphyroclasts of magmatic Ca-pyroxene (augite) that hosts sulphurs and that are partially to totally replaced by coronitic Ca–Na-pyroxene (1; omphacite composition; Fig. 5a, b); fringes of Na-amphibole + pyrite or titanite grow from Ca–Na-pyroxene crystals (1), gradually replacing them (Fig. 5b–f). Ca–Na-pyroxene (2)

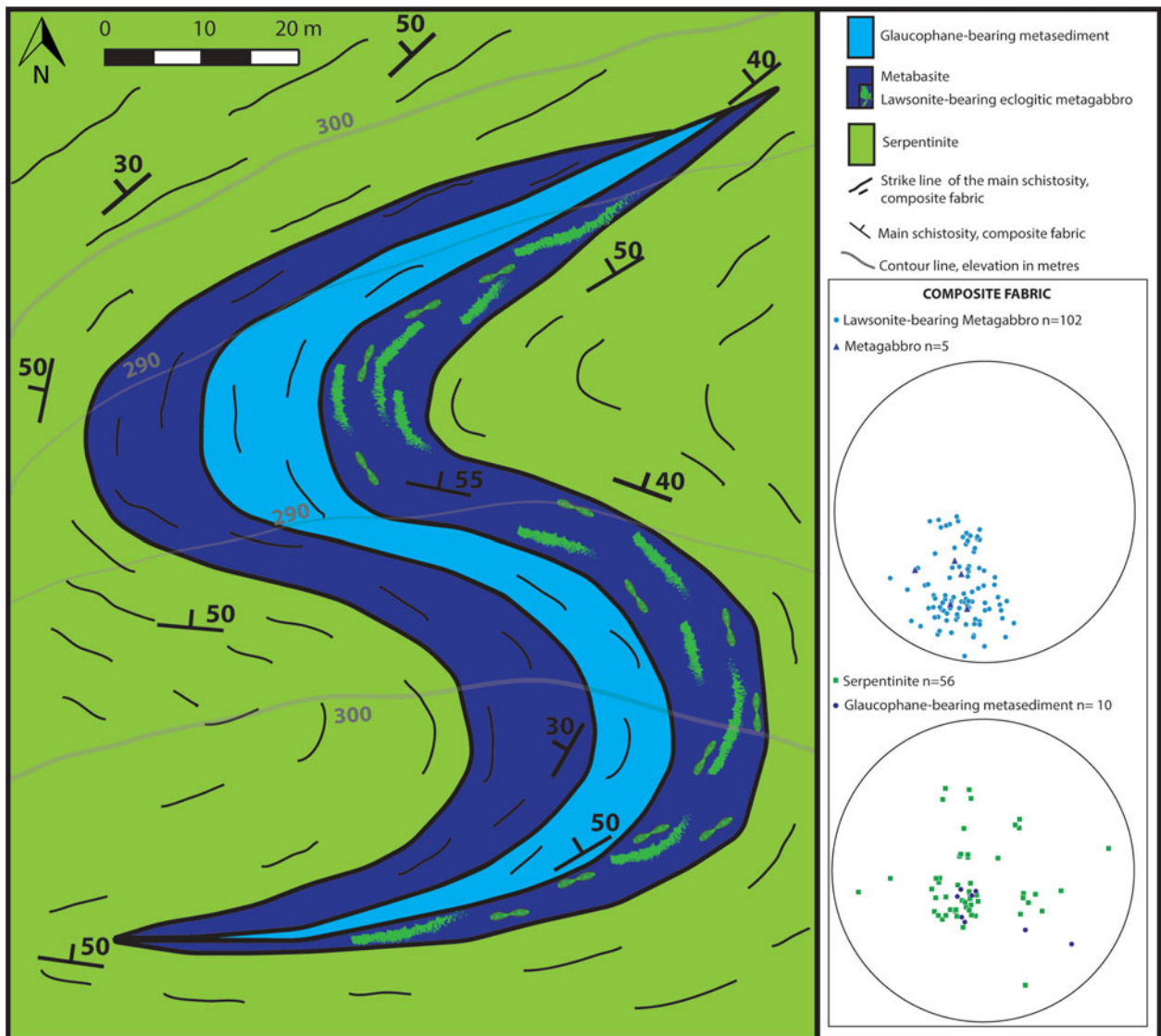


Figure 3. (Colour online) Geological map of the Roboaro River area; the Schmidt nets (lower hemisphere) show the attitude of the composite fabric in different lithotypes.

recrystallizes as syn-kinematic subgrains (Fig. 5a, c, d, e). Rare garnet includes fine-grained Na-amphibole (1) in the core (Fig. 6a) and grows in equilibrium with Ca–Na-pyroxene. Lawsonite nucleates in the Na-amphibole (2) pressure shadows growing from Ca–Na-pyroxene (1) and is replaced by later albite (Figs 5f, 6b).

The Ca–Na-pyroxene layers are overgrown by light-green syn-kinematic fine-grained clinozoisite + minor Na-amphibole (2–3) and white mica (phengite) (Fig. 5d, e). The clinozoisite-rich layers preserve rare garnet that is overgrown by Fe-epidote, glaucophane and chlorite (Fig. 6a).

The blue layers consist of syn-kinematic Na-amphibole (2–3) + minor epidote, white mica (phengite), titanite and Fe-oxide. These layers include porphyroclasts, interpreted as former pyroxene (augite), replaced by fine-grained Na-amphibole (2–3) + clinozoisite + Fe-oxide or showing fringes of Na-

amphibole (2) + white mica and Fe-oxide. Locally relict pyrite, replaced by chalcopyrite, occurs.

Rare layers of fine-grained syn-kinematic titanite, including Fe-oxide and rutile, are preserved.

One main metamorphic peak event, resulting in two assemblages controlled by rock compositional layering, is therefore recorded by the rock (1, 2; Fig. 7): (i) the first assemblage is defined by the static crystallization of Ca–Na-pyroxene (1) + garnet (1) + rutile (1) ± white mica (1) ± Na-amphibole (1) ± lawsonite; (ii) the second one consists of syn-kinematic Ca–Na-pyroxene (2) + garnet (2) + Na-amphibole (2) + rutile (2) + white mica (2) + lawsonite.

These assemblages are replaced by retrograde syn-kinematic Na-amphibole (3) + epidote + white mica (3) + lawsonite + titanite.

The later crystallization event is marked by chlorite, albite and Ca-amphibole growing at the expense of garnet, Ca–Na-pyroxene and Na-amphibole.

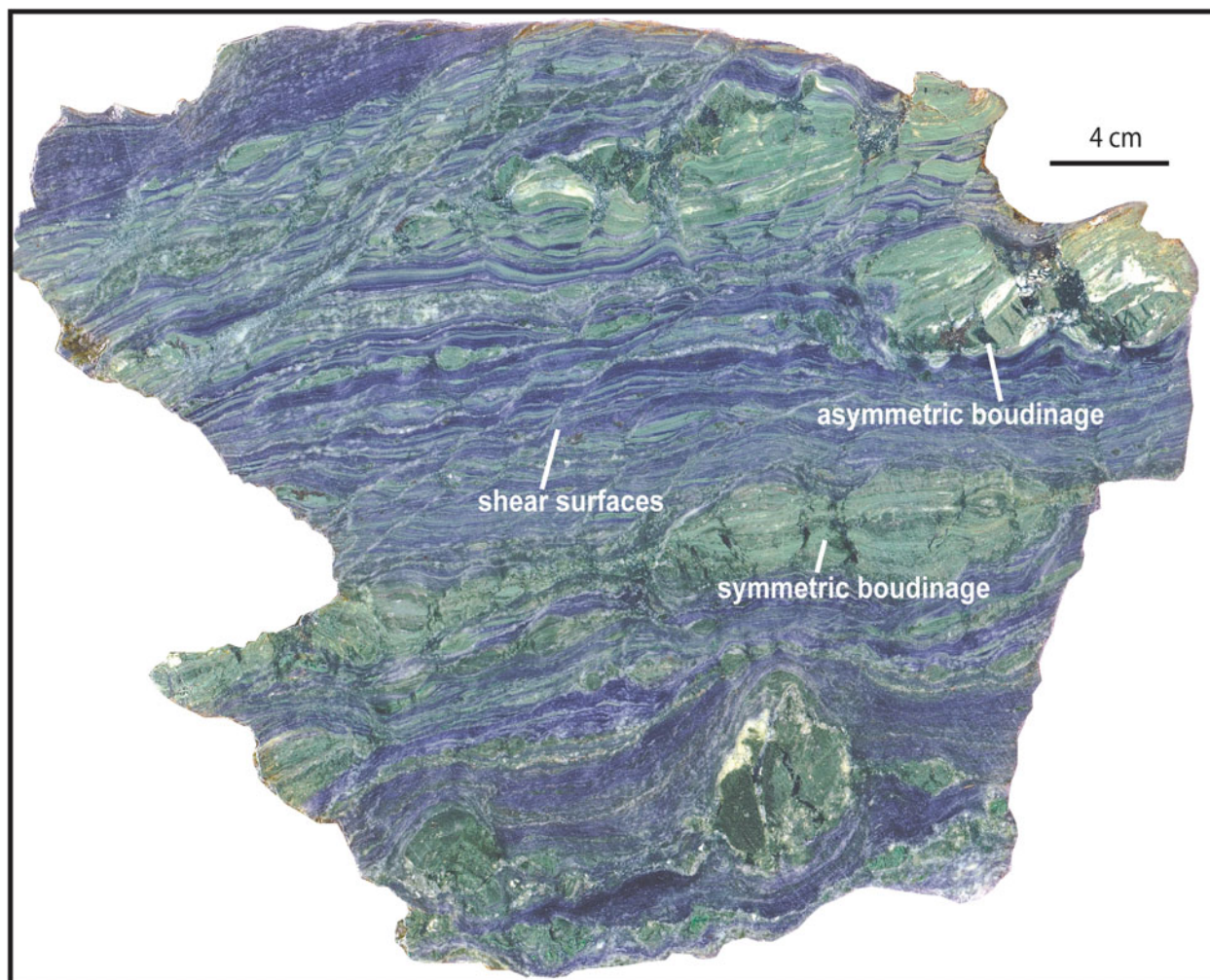


Figure 4. (Colour online) High-resolution scan of a sample from the metagabbro body, showing the peculiar green and blue layering; boudinage of the Ca–Na-pyroxene green layers and low-angle shearing surfaces in Na-amphibole-rich blue layers are visible.

5. Mineral chemistry

We analysed the chemical compositions of the main minerals from the lawsonite-bearing eclogitic metagabbro with an Electron Microprobe (JEOL 8200 Super Probe) at ‘Ardito Desio’ Earth Sciences Department (University of Milan, Italy), using a WDS system. The working conditions were set at 15 kV accelerating voltage and 4.9 nA beam current. Natural minerals were used as standards. Table 1 groups the analyses of representative minerals.

5.a. Amphibole and pyroxene

Amphiboles are present in different proportions both in the green and blue layers. Amphibole chemical analyses have been recalculated on the basis of 24 oxygens and classified as glaucophane and actinolite, according to Hawthorne *et al.* (2012) (Table 1). Glaucophane is found as inclusions in garnet and stable along the main foliation, finally replacing omphacite; Si ranges between 7.98 and 8 atoms per formula unit (a.p.f.u.) and Al_{tot} varies in the range 1.61–1.90 a.p.f.u. The

Ca-amphibole actinolite overgrows garnet, omphacite and glaucophane; Si ranges between 7.55 and 8 a.p.f.u. and Al_{tot} varies in the range 0.09–0.29 a.p.f.u.

Pyroxenes have been classified following Morimoto *et al.* (1988) (Fig. 8a, b; Table 1); relict magmatic Ca-pyroxenes are augites and are in the order of about 1.5–2 mm in size; $Na/(Na + Ca) = 0.04–0.05$. Ca–Na varieties are omphacite and aegirine–augite that grow either on augite, or as fine-grained crystals ($\approx 150–200 \mu m$ sized) along the foliation; in these pyroxenes $Na/(Na + Ca) = 0.26–0.54$.

5.b. Garnet and epidote

Garnet ($\approx 200–250 \mu m$ sized) is almandine-rich (Fig. 8c) and shows glaucophane inclusions ($\approx 10–15 \mu m$ sized) (Fig. 6a). It is compositionally zoned with decreasing Fe and increasing Mn from the core ($X_{Fe^{2+}} = 53$; $X_{Mn} = 18$) to the rim ($X_{Fe^{2+}} = 44$; $X_{Mn} = 26$) (Table 1).

Epidote ($\approx 100–150 \mu m$ sized) grows together with glaucophane (3); it has been classified on the basis of the molar fractions of the end-members

Table 1. Chemical analyses of representative minerals

	Grt					Amph		Ep	Lws	Wm	Pyroxene							
	Core (a)	Mantle (a)	Rim (a)	Core (b)	Rim (b)	Gln	Act				Omph	Agt	Aug					
SiO₂	38.18	38.54	38.26	38.20	38.25	59.41	57.27	SiO₂	40.03	38.49	36.75	37.84	55.83	52.46	SiO₂	56.22	54.96	52.51
TiO₂	0.12	0.10	0.13	0.17	0.10	0.04	0.00	TiO₂	0.02	0.14	0.15	0.00	0.05	0.07	TiO₂	0.05	0.06	0.43
Al₂O₃	21.66	21.63	21.22	21.21	21.92	11.98	0.83	Al₂O₃	34.00	26.26	30.13	31.46	19.65	24.50	Al₂O₃	7.82	5.61	3.03
Cr₂O₃	0.00	0.00	0.01	0.07	0.00	0.01	0.00	Cr₂O₃	0.07	0.05	0.39	0.26	0.00	0.00	Cr₂O₃	0.04	0.86	1.03
FeO	24.76	23.80	20.39	23.98	20.84	6.66	7.79	FeO	0.53	10.14	1.21	0.73	2.00	2.28	FeO	8.04	11.68	4.95
MgO	1.05	0.97	0.79	0.85	0.89	11.99	19.26	MgO	0.00	0.02	0.00	0.17	6.56	4.57	MgO	8.21	7.48	15.84
MnO	8.27	8.49	11.79	9.19	11.91	0.10	0.40	MnO	0.03	0.28	0.00	0.00	0.00	0.04	MnO	0.20	0.18	0.14
CaO	8.88	9.54	9.73	8.75	9.22	0.29	11.32	CaO	23.98	23.28	16.86	17.22	0.04	0.01	CaO	12.31	11.74	21.75
Na₂O	0.04	0.04	0.00	0.06	0.00	7.48	1.02	Na₂O	0.03	0.01	0.00	0.00	0.07	0.24	Na₂O	7.34	7.73	0.59
K₂O	0.00	0.01	0.00	0.00	0.00	0.02	0.10	K₂O	0.00	0.02	0.00	0.00	10.15	9.99	K₂O	0.00	0.01	0.01
SUM	102.96	103.11	102.32	102.48	103.12	97.97	97.99	SUM	98.69	98.69	85.49	87.68	94.35	94.16	SUM	100.24	100.31	100.28
Si	2.98	3.00	3.00	3.02	2.98	7.98	7.99	Si	3.00	3.00	2.01	2.01	3.73	3.52	Si	2.01	1.98	1.92
Ti	0.01	0.01	0.01	0.01	0.01	0.00	0.00	Ti	0.00	0.01	0.01	0.00	0.00	0.00	Al.IV	0.00	0.02	0.08
Al	1.99	1.98	1.96	1.93	2.01	1.90	0.14	Al	3.01	2.41	1.94	1.97	1.55	1.94	Al.VI	0.33	0.22	0.05
Cr	0.00	0.00	0.00	0.00	0.00	0.00	0.00	Cr	0.00	0.00	0.02	0.01	0.00	0.00	Ti	0.00	0.00	0.01
Fe	1.62	1.55	1.34	1.54	1.36	0.75	0.91	Fe	0.03	0.59	0.06	0.03	0.11	0.13	Cr	0.00	0.02	0.03
Mg	0.12	0.11	0.09	0.12	0.10	2.40	4.00	Mg	0.00	0.00	0.00	0.01	0.65	0.46	Fe³⁺	0.16	0.31	0.02
Mn	0.55	0.56	0.78	0.57	0.79	0.01	0.05	Mn	0.00	0.02	0.00	0.00	0.00	0.00	Fe²⁺	0.08	0.04	0.13
Ca	0.74	0.80	0.82	0.82	0.77	0.04	1.69	Ca	1.93	1.94	0.99	0.98	0.00	0.00	Mg	0.44	0.40	0.86
Na	0.01	0.01	0.00	0.00	0.00	1.95	0.28	Na	0.00	0.00	0.00	0.00	0.01	0.03	Ni	0.00	0.00	0.00
K	0.00	0.00	0.00	0.00	0.00	0.00	0.02	K	0.00	0.00	0.00	0.00	0.87	0.86	Mn	0.01	0.01	0.00
Ni	0.00	0.00	0.00	0.00	0.00	0.00	0.00	Ni	0.00	0.00	0.00	0.00	0.00	0.00	Ca	0.47	0.45	0.85
SUM	8.02	8.01	8.01	8.01	8.01	15.04	15.08	SUM	7.98	7.99	5.01	5.01	6.93	6.95	Na	0.51	0.54	0.04
X_{Fe2+}	0.53	0.51	0.44	0.52	0.50			X_{ep}	3	59					K	0.00	0.00	0.00
X_{Ca}	0.25	0.26	0.27	0.24	0.27			X_{czo}	97	41					Sum	4	4	4
X_{Mn}	0.18	0.19	0.26	0.20	0.19										X_{na}	0.52	0.55	0.05
X_{Mg}	0.04	0.04	0.03	0.03	0.04										Q	0.49	0.45	0.96
															Jd	0.34	0.23	0.03
															Ae	0.17	0.32	0.01

$X_{ep} = (Fe/(Fe + (Al(VI) - 2))) * 100$
 $X_{czo} = Al(VI) - 2/(Al(VI) - 2 + Fe) * 100$
 $X_{na} = Na/(Na + Ca)$
 $X_{Fe2+} = Fe^{2+}/(Ca + Mg + Mn + Fe^{2+})$
 $X_{Mn} = Mn/(Ca + Mg + Mn + Fe^{2+})$
 $X_{Mg} = Mg/(Ca + Mg + Mn + Fe^{2+})$
 $X_{Ca} = Ca/(Ca + Mg + Mn + Fe^{2+})$
 $Q = Ca + Mg + (Fe^{2+}/(Fe^{2+} + Mg + Ca + 2Na))$
 $Jd = 2Na * (AlVI/(AlVI + Fe^{3+}))$
 $Ae = 2Na * (Fe^{3+}/(AlVI + Fe^{3+}))$

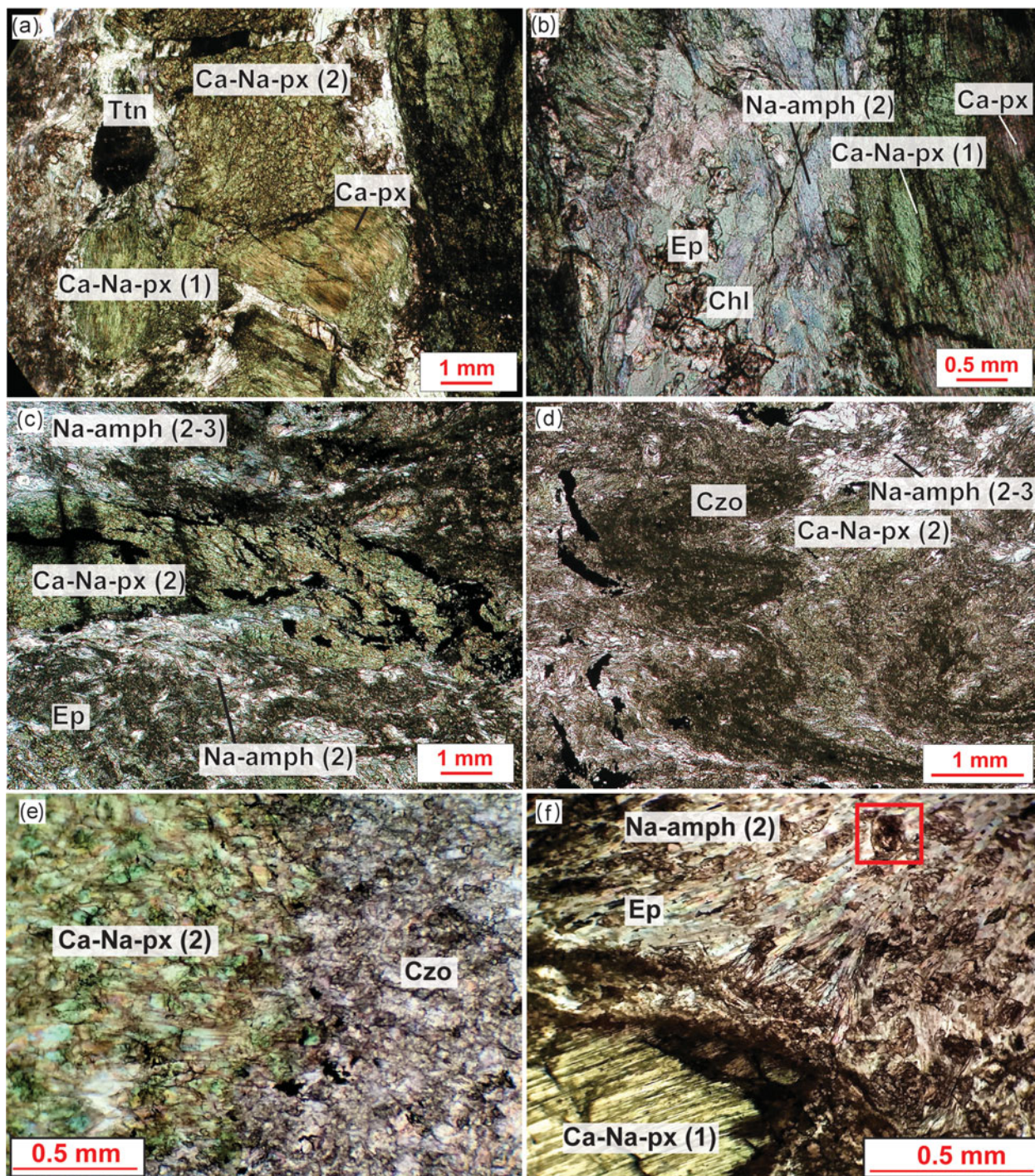


Figure 5. (Colour online) Photomicrographs of representative minerals and structures in the metagabbro. (a) Ca–Na–pyroxene grows first statically replacing magmatic pyroxene relics; Ca–Na–pyroxene later recrystallizes as subgrains (uppermost part of the picture). Na–amphibole overgrows Ca–Na–pyroxene. (b) Porphyroclast of magmatic pyroxene replaced by Ca–Na–pyroxene and by later Na–amphibole. (c) Fold hinge in a Ca–Na–pyroxene-rich layer; here pyroxene forms syn-kinematic subgrains. (d) Folds deforming the Ca–Na–pyroxene-rich and the clinozoisite-rich layers. (e) Epidote replacing Ca–Na–pyroxene. (f) Pressure shadows of glaucophane growing from the Ca–Na–pyroxene; the red box depicts the area shown in Figure 6b, where lawsonite occurs.

in the epidote solid solutions series (clinozoisite and epidote); they were calculated respectively as: $X_{cz} = Al^{(VI)} - 2 / ((Al^{(VI)} - 2) + Fe^{3+})$; $X_{ep} = Fe^{3+} / ((Al^{(VI)} - 2) + Fe^{3+})$.

The chemical composition of epidote varies between the clinozoisite ($X_{ep} = 3$) and the Fe-rich epidote end-members ($X_{ep} = 59$) (Table 1).

5.c. Lawsonite and white mica

Preserved lawsonite ($\approx 10\text{--}15\ \mu\text{m}$ sized) has been classified on the basis of 8 oxygens (Table 1) and shows an almost pure composition with Fe content in the range of 0.02–0.06 a.p.f.u.; it grows in pressure shadows (around Ca–Na–pyroxene) made of glaucophane and is replaced by later albite.

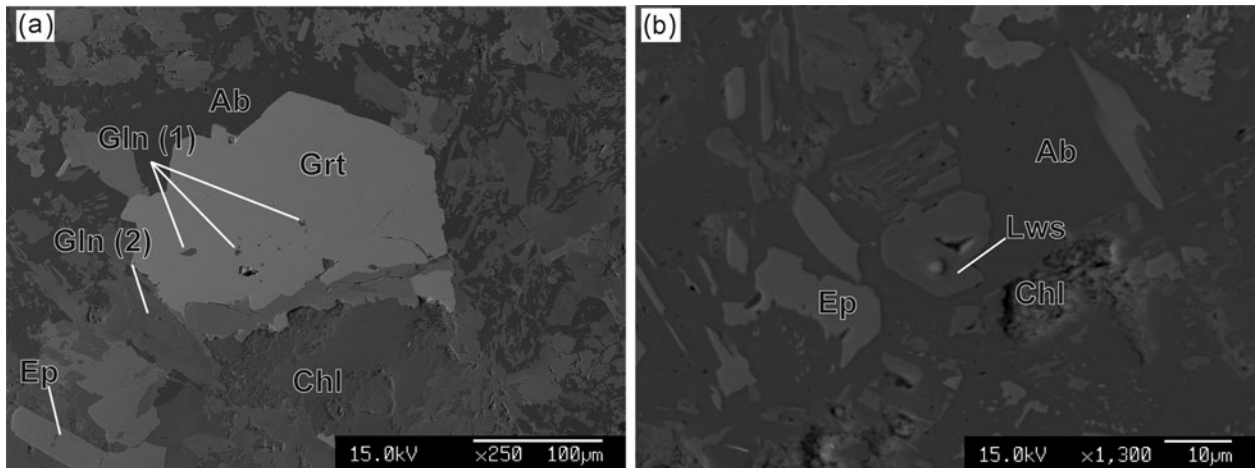


Figure 6. (a) Back-scattered electron (BSE) image of a garnet crystal replaced by epidote, chlorite and albite. (b) BSE image of a lawsonite crystal surrounded by albite; the dot inside the lawsonite crystal is the analysis point.

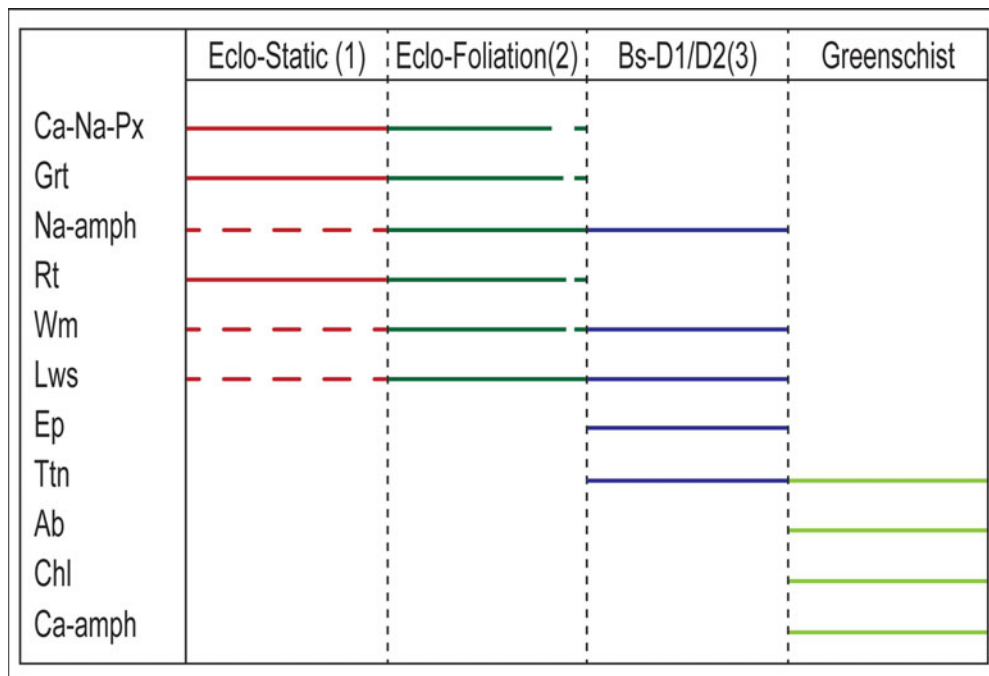


Figure 7. (Colour online) Phase crystallization diagram showing the minerals stability along the metamorphic path. Eclo – eclogitic facies; Bs – blueschist facies; the progressive numbers represent the parageneses; D1 and D2 are the two main deformational events.

White mica composition has been calculated on the basis of 11 oxygens and considering iron as Fe^{2+} . White mica occurs as fine-grained crystals of phengite with Si content ranging between 3.55 and 3.77 a.p.f.u. and $(\text{Mg} + \text{Fe}_{\text{tot}}) = 0.59\text{--}0.77$ a.p.f.u.; the phengite compositions lie very close to the celadonite–muscovite compositional joint, reflecting the important role of Tschermak's substitution and confirming that almost no Fe^{3+} occurs (Vidal & Parra, 2000; Groppo *et al.* 2016).

6. P – T estimates

We used a thermodynamic modelling approach to assess the P – T evolution of the metagabbro body and to constrain its metamorphic peak conditions. P – T

pseudosections were calculated using Perple_X (<http://www.perplex.ethz.ch>; Connolly, 1990) for the system KMnTiNCFMASH with H_2O considered in excess ($a_{\text{H}_2\text{O}} = 1$) (Table 2).

The bulk-rock composition of the rock was determined by inductively coupled plasma mass spectrometry (ICP-MS) analysis at Activation Laboratories Ltd (Ontario, Canada). The thermodynamic dataset and equation of state for H_2O – CO_2 fluid of Holland & Powell (1998, revised 2002) were implemented. We used the following solid solutions: garnet (Holland & Powell, 1998), amphibole (Wei & Powell, 2003; White, Powell & Phillips, 2003), omphacite (Holland & Powell, 1996), chlorite (Holland, Baker & Powell, 1998), phengite (Holland & Powell, 1998) and epidote (Holland & Powell, 1998).

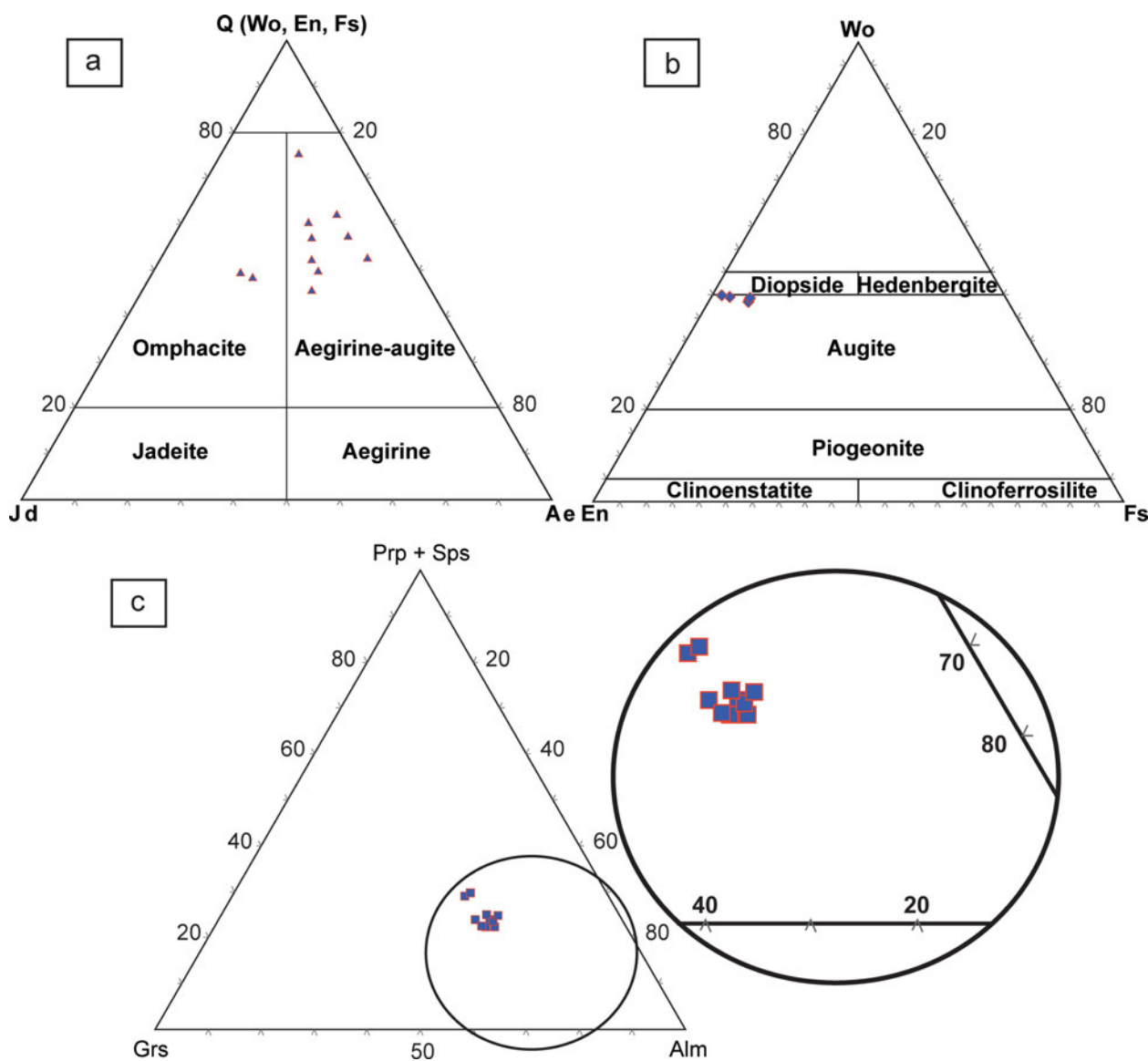


Figure 8. (Colour online) Classification diagrams of representative minerals. (a, b) Na- + Ca-Na- and Ca-Mg-Fe-pyroxene, respectively (after Morimoto *et al.* 1988). (c) Garnet classification diagram.

Table 2. Bulk-rock compositions of sample SC37 (lawsonite-bearing metagabbro)

Weight %	Detection limit	SC37 <i>H₂O excess</i>	SC37 <i>With LOI</i>
SiO ₂	0.01	50.31	48.13
Al ₂ O ₃	0.01	17.89	17.11
FeO	0.01	7.34	7.02
MnO	0.001	0.12	0.11
MgO	0.01	8.98	8.59
CaO	0.01	10.87	10.40
Na ₂ O	0.01	3.72	3.56
K ₂ O	0.01	0.06	0.06
TiO ₂	0.001	0.72	0.69
LOI		0.00	4.33
Total		100	100

Since the used analytical method for defining the bulk-rock composition cannot estimate the real proportion between ferrous and ferric iron, and in order to account for the occurrence of epidote, we

simulated pseudosections with various hypothetical Fe³⁺ amounts (i.e. Fe₂O₃ = 10% – 20% Fe_{tot}). The compositional isopleths calculated for garnet cores in the pseudosections with Fe₂O₃ = 10% – 20% Fe_{tot} diverged from each other suggesting that the considered bulk composition did not fit the rock composition during garnet growth. We thus neglected Fe³⁺ and simulated the pseudosection shown in Figure 9a and Figure S1 (online Supplementary Material available at <http://journals.cambridge.org/geo>) that includes tri- to esavariant fields. The compositional isopleths calculated for garnet cores ($X_{\text{Fe}^{2+}} = 0.53$, $X_{\text{Ca}} = 0.25$, $X_{\text{Mn}} = 0.18$, $X_{\text{Mg}} = 0.04$) in the free-Fe³⁺ pseudosection define their growth conditions in the range 465–477 °C and 20.9–24.4 kbar and cross-cut into the field where chl + Ca-Na-px + wm + 2 Na-amph + grt + lws + rt occur (the mineral abbreviations are after Kretz, 1983, except for Ca-Na-px = Ca-Na-pyroxene, Na-amph = Na-amphibole and wm = white mica). This confirms that the amount of Fe³⁺ in

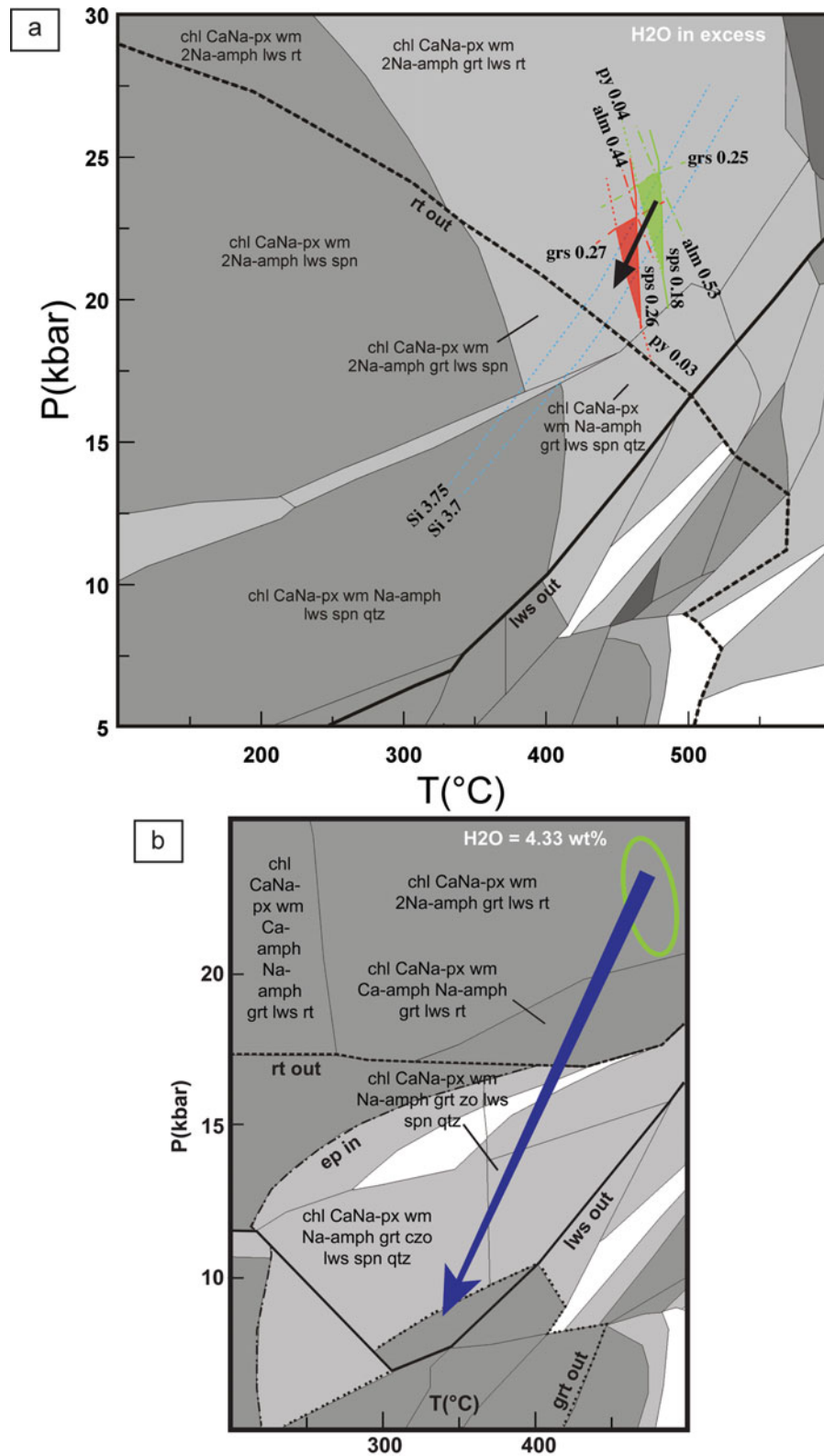


Figure 9. (Colour online) P – T pseudosections in the KMnTiNCFMASH system. The mineral abbreviations are after Kretz (1983) except for: cpx – clinopyroxene; Na-amph – Na-amphibole; Ca-amph – Ca-amphibole; wm – white mica; and Ca–Na-px – Ca–Na-pyroxene. Narrow and small fields have been ignored for the sake of clarity. (a) P – T pseudosection with H_2O in excess. The stability conditions of the garnet core and rim are shown by green and red fields, respectively. The dotted light blue lines are isopleths of Si in white mica. The arrow shows the first stage of the retrograde path along a $3\text{ }^\circ\text{C km}^{-1}$ gradient. (b) P – T pseudosection with under-saturated conditions ($H_2O = \text{LOI}$). The peak metamorphic conditions are highlighted by the green circle. The blue arrow depicts the later stages of the retrograde path with coexisting lawsonite and epidote.

the rock is closer to 0% Fe_{tot} than to 10% Fe_{tot}. The compositional isopleths of Si in mica (Si = 3.70–3.75 a.p.f.u.) fit the isopleths of the garnet core testifying to the growth of high-pressure mica. In the pseudosection, the amount of chlorite at the *P–T* conditions defined by garnet growth is 13 wt%. The occurrence in our sample of chlorite stable at peak metamorphic conditions is difficult to estimate, since chlorite recrystallized at lower *P–T* conditions, probably erasing its former stability relations. The mineralogical association described in the above field, however, well represents the metamorphic peak assemblage that we observe in the rock; this field also includes lawsonite, which is presently observed in the Na-amphibole pressure shadows growing from Ca–Na-pyroxene. Since the garnet chemical zonation is minor, we think that the fractionation effect on the bulk composition of the system is very low; we thus used the composition of the garnet rim to trace the *P–T* evolution of the rock. The compositional isopleths of the garnet rim (X_{Fe2+} = 0.44, X_{Ca} = 0.27, X_{Mn} = 0.26, X_{Mg} = 0.03) constrain the growing conditions at about 448–465 °C and 19.3–22.8 kbar, at lower *P–T* compared to the one predicted by the garnet core.

The *P–T* fields derived from the stability conditions of the garnet core and rim (Fig. 9a) define a possible initial retrogression path of the eclogitic metagabbro body (arrow in Fig. 9a) along a very low thermal gradient (3 °C km⁻¹). This value (i.e. 3 °C km⁻¹) results from the thermobaric gradient of the path later transformed, according to the lithostatic pressure (0.3 kbar km⁻¹), into a thermal gradient.

The later retrogressive stages are defined in our rock by the coexistence of lawsonite, Na-amphibole and epidote; this assemblage is, however, not represented in the fields of the pseudosection that we calculated with H₂O in excess. To understand the possible role of H₂O in the stability of this retrograde assemblage, we calculated the stability fields for the free-Fe³⁺ bulk-rock composition along the geotherm defined for the above exhumation path (i.e. 3 °C km⁻¹). The *P/T* X(H₂O) pseudosection (Fig. S2, online Supplementary Material available at <http://journals.cambridge.org/geo>) shows that, in order to obtain the simultaneous stability of lawsonite and epidote, under-saturated conditions should occur. The transition from H₂O in excess (at peak metamorphic conditions) to under-saturated conditions (during the retrograde path) could be explained with H₂O request by lawsonite during its growth; the subtraction of H₂O from the system (i.e. under-saturated system) allowed the simultaneous occurrence of lawsonite and epidote in the system as observed by Poli & Schmidt (1997). This has been extensively evaluated using pseudosections by Balleve, Pitra & Bohn (2003), López-Carmona, Pitra & Abati (2013), López-Carmona *et al.* (2014) and Groppo *et al.* (2016).

The *P–X*(CO₂) pseudosection (Fig. S3, online Supplementary Material available at <http://journals.cambridge.org/geo>), calculated at *T* = 400 °C, reveals that lawsonite is stable in the range *P* = 11–25 kbar, for

X(CO₂) < 0.015 (with X(CO₂) = CO₂ / (CO₂ + H₂O)); for X(CO₂) in the range 0.0013–0.015 lawsonite occurs together with carbonates.

Since in our samples we observed the sole presence of lawsonite (without carbonates), according to the above *P–X*(CO₂) pseudosection, X(CO₂) in the fluid should be < 0.13 % of the total loss on ignition (LOI). To trace the retrograde exhumation path we thus neglected CO₂ and simulated an under-saturated system considering the LOI (LOI = 4.33 wt%) as pure water (Fig. 9b and Fig. S4 in the online Supplementary Material available at <http://journals.cambridge.org/geo>).

The path in Figure 9b passes through fields where lawsonite coexists with epidote, crossing the rutile breakdown reaction (*P* < 15 kbar).

The metagabbro body thus experienced different H₂O contents: at eclogitic metamorphic peak conditions (*T* = 465–477 °C and *P* = 20.9–24.4 kbar), H₂O was continuously supplied to the system, allowing lawsonite formation; the retrograde history was marked by the decrease of water content and under-saturated conditions, with the occurrence of both lawsonite and epidote.

7. Discussion

7.a. Occurrence of a lawsonite-bearing eclogitic metagabbro in the Voltri Massif

The lawsonite-bearing eclogitic metagabbro (Ca–Na-px + garnet + gln + rt + ph + lws) studied in this paper is an unusual lithology, as lawsonite is rarely preserved in a strongly deformed rock that records high-pressure metamorphic peak conditions, as the studied metagabbro is. Davis & Whitney (2006) and Vitale Brovarone *et al.* (2011) in fact proposed that fresh lawsonite eclogites are preserved only in domains unaffected by post-eclogitic deformation, which prevents high-pressure mineral retrogression; we, however, observed that lawsonite grows also along the mylonitic foliation in Ca–Na-pyroxene pressure shadows. Lawsonite-bearing eclogites are reported only in a few outcrops of the Voltri Massif: lawsonite occurs as pseudomorphs replaced by aggregates of epidote + paragonite + chlorite ± phengite in eclogitic metagabbro of the eastern sector of the Voltri Massif (i.e. Mt Pesucco outcrop, Malatesta *et al.* 2012a; ‘Prato del Gatto’ and ‘Case Buzzano’ eclogitic metagabbro, Capponi & Crispini, 2008a).

In the Cascine Parasi outcrop, about 3.5 km distance from our study zone, eclogite metagabbro boulders in a tectonic *mélange* show high-pressure assemblages with preserved stable lawsonite (Federico *et al.* 2007b). In the same outcrop, eclogite metagabbro and metasediment bodies include aggregates interpreted as pseudomorphs after lawsonite (Cortesogno *et al.* 1981; Federico *et al.* 2007b).

Most of the worldwide lawsonite eclogites are blocks intimately associated with serpentinites, as in our case; some of them are instead coherent units

associated with blueschist, orthogneiss or paragneiss (Tsujimori *et al.* 2006a and references therein; Vitale Brovarone *et al.* 2011). The assemblage observed in our lawsonite-bearing eclogitic metagabbro and the estimated metamorphic peak conditions ($T = 465\text{--}477\text{ }^{\circ}\text{C}$ for $P = 20.9\text{--}24.4$ kbar) are comparable with what is observed in worldwide lawsonite eclogites in serpentinites; they usually preserve a general prograde assemblage with grt + omp + lws + wm + qtz ± rt ± ttn ± gln ± chl ± tlc, recording peak pressure in the range 14–30 kbar and temperature between 360 and 570 °C (Tsujimori *et al.* 2006a,b; Tsujimori & Ernst, 2014 and references therein; Davis & Whitney, 2006). We have little evidence about the prograde path of our samples, except for glaucophane inclusions in garnet, that testify to its possible occurrence also at metamorphic peak conditions. Eclogites and eclogitic metabasalts of Alpine Corsica show metamorphic peak assemblages (grt + omp + ph + gln + lws + qtz + ttn + opq, Ravna *et al.* 2010 and references therein; omp + lws + grt + ph + ttn ± gln ± act ± chl, Vitale Brovarone *et al.* 2011; abbreviations are after Whitney & Evans, 2010) stable at *c.* 390 °C at 2.05 GPa for eclogites, and 340–415 °C, 1.9–2.6 GPa (Ravna *et al.* 2010) or 520 ± 20 °C and 2.3 ± 0.1 GPa, for the eclogitic metabasalts (Vitale Brovarone *et al.* 2011).

The peak assemblages proposed for the Roboaro lawsonite-bearing eclogitic metagabbro are particularly similar to lawsonite eclogites from South Motagua (Guatemala; Tsujimori *et al.* 2006b), the Central Pontides (Turkey; Altherr *et al.* 2004) and the Sivrihisar Massif (Turkey; Davis & Whitney, 2006), even if the stability conditions are mostly comparable to the South Motagua lawsonite eclogites (1.8–2.5 GPa and 290–470 °C).

The development and preservation of lawsonite in rocks that experienced high-pressure conditions requires both cold subduction and a rapid exhumation (Tsujimori *et al.* 2006a,b; Çetinkaplan *et al.* 2008). Lawsonite is an important carrier of water and trace elements to high depths (at least 300 km in cold subduction zones): it accommodates up to 11.5 wt% of H₂O that can be released from the slab, providing volatiles for arc magmatism and subduction zone seismicity (Schmidt & Poli, 1998; Tsujimori *et al.* 2006a,b and references therein).

The preservation of lawsonite in the rocks along the Roboaro River suggests that at least one of these conditions (i.e. cold subduction and rapid exhumation) has been verified. Concerning the first hypothesis (i.e. cold subduction), thermodynamic modelling suggests that the metagabbro body reached peak metamorphic conditions at a relatively low temperature ($T = 465\text{--}477\text{ }^{\circ}\text{C}$ for $P = 20.9\text{--}24.4$ kbar), in a setting where H₂O was continuously provided to a cold system. Spandler & Pirard (2013) suggested that the maximum P – T conditions reached by lawsonite eclogites may not necessarily reflect the general conditions of cold subduction: as the shallow fore-arc mantle is

cooler than the deep sub-arc mantle wedge, the top of the subducting slab undergoes rapid heating after coupling with the hot asthenospheric mantle wedge. The preservation of lawsonite eclogite can suggest that they were exhumed prior to heating of the slab by the overlying asthenosphere and were not related to a general cold subduction.

Concerning the exhumation rate, even if a rapid exhumation has been proposed for the preservation of lawsonite in high-pressure rocks Tsujimori *et al.* (2006a), Agard *et al.* (2009) suggested that lawsonite can survive at slow exhumation rates if refrigerant conditions are maintained. Proposed exhumation rates for eclogite and blueschist rocks of the Voltri Massif range from 3.3–3.9 mm y⁻¹ (Federico *et al.* 2005) to 25 mm y⁻¹ (Rubatto & Scambelluri, 2003); the latter velocity has been recalculated by C. Malatesta (unpub. Ph.D. thesis, Univ. degli Studi di Genova, 2011) and attests to values of 10–12 mm y⁻¹, considering an exhumation time of 4 Ma. The exhumation rates proposed for the Voltri Massif are therefore in general low values and seem to confirm that lawsonite is preserved thanks to cold conditions during subduction rather than a rapid exhumation.

7.b. CO₂-rich fluids and fluid–rock interaction

The occurrence of carbonated serpentinites, wrapping the eclogitic metagabbro and metasediment bodies, suggests that an intense and long-lasting circulation of CO₂-rich fluids affected the area around the Roboaro River and the adjacent zones. The country-rock serpentinites show various degrees of carbonation until their complete transformation into listvenites. Serpentinites are replaced by carbonate minerals starting preferentially from veins that either follow the pervasive foliation or from mesh structures; carbonates also grow along late fracture systems. All these structures acted as preferential pathways for the infiltration of CO₂-bearing fluids during subduction.

The occurrence of listvenites and carbonated serpentinites mainly along fault zones (Fig. 1b) also confirms the structural control of fluid circulation along shear zones and the damage zone of faults.

Further evidence on the circulation of CO₂-rich fluids comes from an outcrop some hundreds of metres from the Roboaro River study area (i.e. La Pesca locality). At this site, Cortesogno, Galbiati & Principi (1980), Cortesogno, Lucchetti & Massa (1981) and Scambelluri *et al.* (2016) described a garnet-bearing marble interlayered with serpentinite, dolomite and hybrid-rocks (the latter intermediate between serpentinite and marble). These rocks have been interpreted either as ophicarbonates bodies formed on an ancient ocean-floor (Cortesogno, Galbiati & Principi, 1981) or as a serpentinite–marble contact; in both cases these rocks were highly deformed and metamorphosed during the high-pressure subduction history (Scambelluri *et al.* 2016). Studying these rocks, Scambelluri *et al.* (2016) hypothesized that CO₂ fluid circulation, and

therefore the formation of high-*P* ophicarbonates, was linked to the dehydration of serpentinite close to metamorphic peak conditions; the released aqueous fluids triggered the breakdown of dolomite in the nearby marbles and this reaction discharged C into the fluids.

In the Roboaro River study area, we have no direct analogies with the outcrop cited above and therefore we do not have clear constraints about the timing of CO₂ fluid circulation into the serpentinites.

No evidence (e.g. carbonates, carbonate-bearing veins) of a strong interaction of the CO₂-rich fluids with the lawsonite-bearing eclogitic metagabbro at high-pressure conditions occurs; this is in accordance with the results of the pseudosections calculation (Section 6; Fig. S4, online Supplementary Material available at <http://journals.cambridge.org/geo>), suggesting that lawsonite is stable in the system for very low contents of CO₂ (i.e. X(CO₂) < 0.13 wt %).

At the current state of knowledge of the area, the reasons why the lawsonite-bearing eclogitic metagabbro escaped from an intense CO₂ fluid circulation are still puzzling; nonetheless some reasonable scenarios could be envisaged: (i) the lawsonite-bearing eclogitic metagabbro and host-rocks have contrasting rheologies and permeabilities; (ii) the lithotypes (i.e. eclogitic metagabbro versus serpentinite) are characterized by different chemical affinities with CO₂-bearing fluids; (iii) the CO₂-bearing fluid circulation pre-dated the coupling of the lawsonite-bearing eclogitic metagabbro with serpentinite.

7.c. Geodynamic implications

The area along the Roboaro River is an example of a hydrated slab portion where both aqueous fluids and carbonate-rich fluids were active. This area of the Voltri Massif recorded multiple superposed deformations, related to a general shear regime. The alternation of Na-amphibole-rich and Ca–Na-pyroxene-rich layers in the eclogitic metagabbro body and the concurrent interfolding of the metagabbro with the metasediment lens and serpentinite are one of the most evident effects of deformation (Fig. 10).

Na-amphibole-rich and Ca–Na-pyroxene-rich layers could derive, respectively, from the hydrous rim and the anhydrous core of mafic lenses incorporated inside serpentinite country-rock, as suggested for metabasalts of the Zermatt-Saas ophiolite by Angiboust & Agard (2010). At the present stage, it is not possible to assess if the amphibole-rich rim reflects an oceanic stage of hydration of the outermost rim of mafic bodies inside the ultramafic serpentinitized basement, or a later interaction of the boudinaged mafic bodies with fluids during the subduction path.

The ductile shear regime that affected this area strongly acted at least from eclogite-facies metamorphic conditions inside the subduction zone, deforming the Ca–Na-pyroxene + garnet association in the metagabbro, and continued to be active at

blueschist-facies conditions, during the exhumation stage. The shear regime also enhanced the circulation of CO₂-rich fluids through the country-rock serpentinite, triggering its partial to total carbonation and transformation into listvenite. The following brittle–ductile structures affecting the metagabbro (i.e. boudinage and low-angle shearing surfaces) formed during late-stage greenschist-facies conditions.

The occurrence of preserved lawsonite coupled with the petrological study suggest that this area underwent different *P–T* conditions (lower *T*) compared to most of the Voltri Massif, where eclogite metagabbros record in general a peak temperature higher than 500 °C (Scambelluri *et al.* 1991; Federico *et al.* 2004; Vignaroli *et al.* 2005); exceptions are the eclogites studied by Liou *et al.* (1998) and Brouwer, Vissers & Lamb (2002), that record *T* = 450 °C for *P* = 18 kbar, and the eclogite studied by Malatesta *et al.* (2012a), with peak *T* = 460–500 °C and *P* = 22–28 kbar; in all these cases, however, lawsonite is absent or is destabilized and occurs as pseudomorphs, suggesting that these eclogites followed hotter exhumation paths.

Accordingly to what was proposed by Spandler & Pirard (2013) for lawsonite-bearing high-pressure rocks, this area could represent a portion of the top of the subducted slab, close to the plate interface: this slab portion was coupled with a hydrated and ‘cool’ mantle wedge that kept our eclogitic metagabbro in a low-temperature regime with the preservation of lawsonite.

The different *P–T* paths identified for the eclogites of the Voltri Massif confirm that it is made up by rock bodies subducted to various depths and brought to the surface along different exhumation trajectories. Moreover, the occurrence of rocks with different paleogeographic origins (e.g. ocean versus continent) in a serpentinite matrix requires a large-scale mechanism that could associate them. As suggested by Federico *et al.* (2007a) and Malatesta *et al.* (2012a,b), the geodynamic mechanism responsible for these kinds of assemblages and their evolution could be involvement in a low-viscosity serpentinite channel close to the plate interface.

8. Main remarks

This work presents a detailed structural, petrographical and petrological study of the Roboaro River area (Voltri Massif, Ligurian Western Alps). The occurrence of a lawsonite-bearing eclogite folded together with metasediments and variously carbonated serpentinites allowed us to interpret this area as an example of a highly hydrated slab portion, where both aqueous fluids and carbonate-rich fluids were present at high-pressure conditions.

The lawsonite-bearing metagabbro body reached eclogitic metamorphic peak conditions at *T* = 465–477 °C and *P* = 20.9–24.4 kbar, with H₂O continuously supplied to the system. The exhumation path was

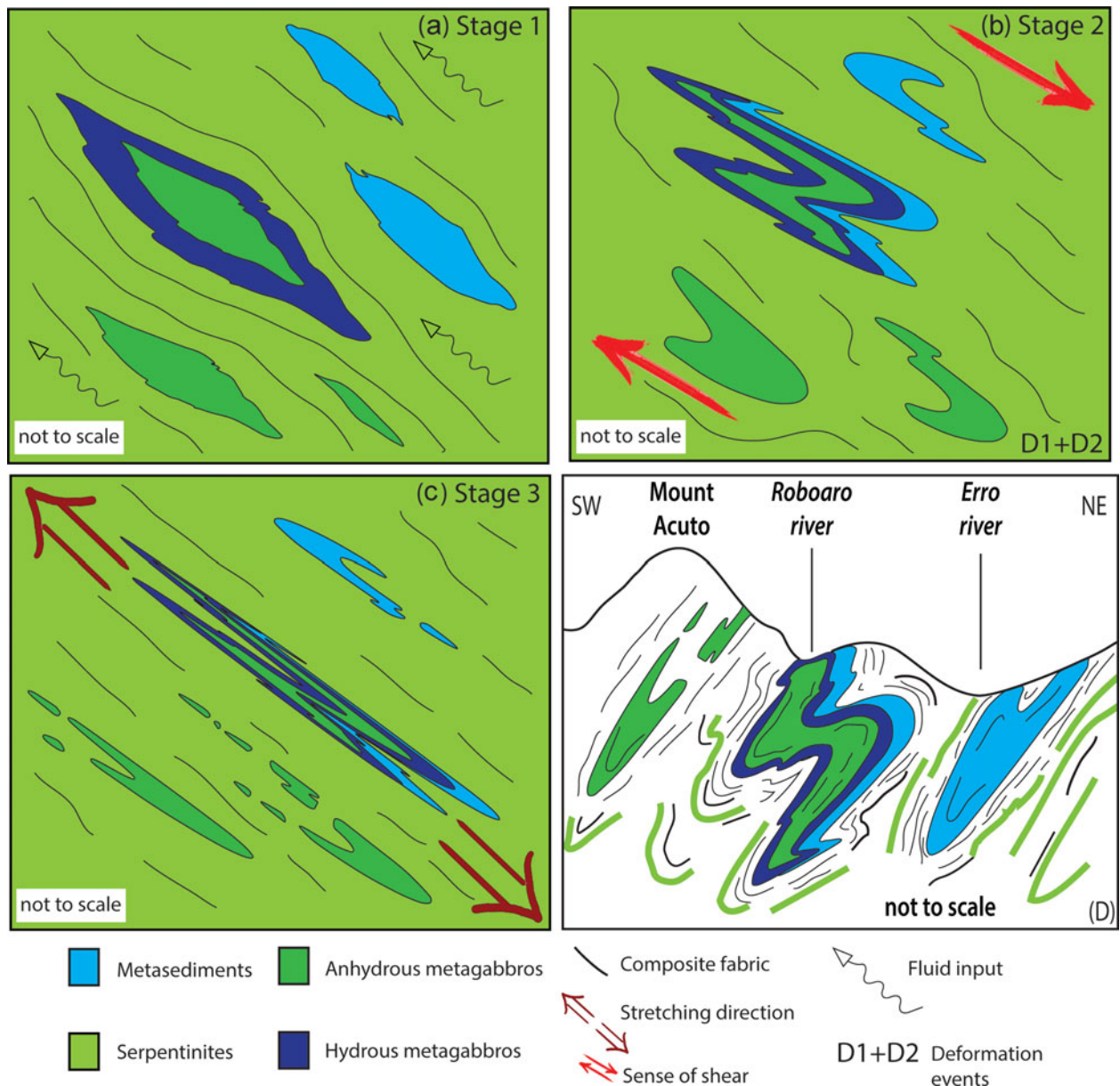


Figure 10. (Colour online) Schematic model of the progressive deformation of the study area. (a) Stage 1: metagabbro and metasediment lenses surrounded by serpentinites with circulating fluids. (b) Stage 2: Progressive deformational events linked with the metamorphic peak and exhumation stages that produced the alternating blue and green layering. (c) Stage 3: Later stretching of the metagabbro body that caused the boudinage of the green layer. (d) Interpretative schematic geological cross-section through the lawsonite-bearing metagabbro body.

characterized by H_2O under-saturated conditions, with the occurrence of both lawsonite and epidote.

The low temperature recorded by the lawsonite-bearing eclogitic metagabbro body led us to interpret this area as a portion of the top of the subducted slab coupled with the hydrated and 'cool' mantle wedge.

Both the multiple deformations recorded during the whole studied history of the body and the occurrence in the area of rocks with different paleogeographic origins (e.g. ocean versus continent), wrapped in a serpentinite matrix, witness that this sector was close to the slab–mantle interface that evolved in a shear regime. These rocks were merged within a low-viscosity serpentinite channel that brought them back to the surface.

Acknowledgements. We greatly appreciate the discussion with Laura Crispini, Laura Federico and Giovanni Capponi; we acknowledge Nicholas Vaiarini for the field assistance. We also thank Andrea Festa, Alicia López-Carmona and Idael Francisco Blanco-Quintero for their detailed and constructive comments which improved this manuscript. This work was financially supported by PRIN 2010 project 'Nascita e morte dei bacini oceanici: processi geodinamici dal rifting alla collisione continentale negli Orogeni mediterranei e circum-mediterranei', national Coordinator G. Capponi.

Supplementary material

To view supplementary material for this article, please visit <https://doi.org/10.1017/S0016756817000395>.

References

- AGARD, P., AMATO, P., JOLIVET, L. & BUROV, E. 2009. Exhumation of oceanic blueschists and eclogites in subduction zones: timing and mechanisms. *Earth-Science Reviews* **92**, 53–79.
- AGUE, J. J. & NICOLESCU, S. 2014. Carbon dioxide released from subduction zones by fluid-mediated reactions. *Nature Geoscience* **7**, 355–60.
- ALTHERR, R., TOPUZ, G., MARSCHALL, H., ZACK, T. & LUDWING, T. 2004. Evolution of a tourmaline-bearing lawsonite eclogite from Elekdag area (Central Pontides, N Turkey): evidence for infiltration of slab-derived B-rich fluids during exhumation. *Contributions to Mineralogy and Petrology* **148**, 409–25.
- ANGIBOUST, S. & AGARD, P. 2010. Initial water budget: the key to detaching large volumes of eclogitized oceanic crust along the subduction channel? *Lithos* **120**, 453–74.
- BALLEVRE, M., PITRA, P. & BOHN, M. 2003. Lawsonite growth in the epidote blueschists from the Ile de Groix (Armorican Massif, France): a potential geobarometer. *Journal of Metamorphic Geology* **21**, 723–35.
- BROUWER, F. M., VISSERS, R. L. M. & LAMB, W. M. 2002. Metamorphic history of eclogitic metagabbro blocks from a tectonic mélange in the Voltri Massif, Ligurian Alps, Italy. *Ophioliti* **27**, 1–16.
- BRUN, J. P. & FACCENNA, C. 2008. Exhumation of high-pressure rocks driven by slab rollback. *Earth and Planetary Science Letters* **272**, 1–7.
- CANNAO, E., SCAMBELLURI, M., AGOSTINI, A., TONARINI, S. & GODARD, M. 2016. Linking serpentinite geochemistry with tectonic evolution at the subduction interface: the Voltri Massif case study (Ligurian Western Alps, Italy). *Geochimica et Cosmochimica Acta* **190**, 115–33.
- CAPPONI, G. 1987. Alcune considerazioni sul Massiccio di Voltri (Alpi Liguri). *Bollettino della Società Geologica Italiana* **106**, 633–45.
- CAPPONI, G. 1991. Megastructure of the south-eastern part of the Voltri Group (Ligurian Alps): a tentative interpretation. *Bollettino della Società Geologica Italiana* **110**, 391–403.
- CAPPONI, G. & CRISPINI, L. 1997. Progressive shear deformation in the metasediments of the Voltri Group (Ligurian Alps, Italy): occurrence of structures recording extension parallel to the regional foliation. *Bollettino della Società Geologica Italiana* **116**, 267–77.
- CAPPONI, G. & CRISPINI, L. 2002. Structural and metamorphic signature of alpine tectonics in the Voltri Massif (Ligurian Alps, northwestern Italy). *Eclogae Geologicae Helvetiae* **95**, 31–42.
- CAPPONI, G. & CRISPINI, L. 2008a. *Note Illustrative della Carta Geologica d'Italia alla scala 1: 50.000 Foglio 213 Genova*. Firenze: SELCA.
- CAPPONI, G. & CRISPINI, L. 2008b. *Carta Geologica d'Italia alla scala 1:50000, Foglio 213 – 230 "Genova"*. Apat – Regione Liguria. Firenze: SELCA.
- CAPPONI, G., GOSSO, G., SCAMBELLURI, M., SILETTO, G. & TALLONE, S. 1994. Carta Geologica – Strutturale del settore centro meridionale del Gruppo di Voltri (Alpi Liguri) e note illustrative. *Bollettino della Società Geologica Italiana* **113**, 383–94.
- CARON, J. M. & PÉQUIGNOT, G. 1986. The transition between blueschist and lawsonite-bearing eclogites based on observations from Corsican metabasalts. *Lithos* **19**, 205–18.
- CARSWELL, D. A. 1990. *Eclogite Facies Rocks*. Berlin: Springer.
- CARSWELL, D. A., TUCKER, R. D., O'BRIEN, P. J. & KROGH, T. E. 2003. Coesite micro-inclusions and the U/Pb age of zircons from the Hareidland eclogite in the Western Gneiss Region of Norway. *Lithos* **67**, 181–90.
- ÇETINKAPLAN, M., CANDAN, O., OBERHÄNSLI, R. & BOUSQUET, R. 2008. Pressure–temperature evolution of lawsonite eclogite in Sivrihisar; Tavşanlı Zone–Turkey. *Lithos* **104**, 12–32.
- CHIESA, S., CORTESOGNO, L., FORCELLA, F., GALLI, M., MESSIGA, B., PASQUARE, G., PEDEMONTE, G. M., PICCARDO, G. B. & ROSSI, P. M. 1975. Assetto strutturale ed interpretazione geodinamica del Gruppo di Voltri. *Bollettino della Società Geologica Italiana* **94**, 555–82.
- COMPAGNONI, R. & MAFFEO, B. 1973. Jadeite-bearing metagranites l.s. and related rocks in the Mount Mucrone area (Sesia-Lanzo Zone, Western Italian Alps). *Schweizerische Mineralogische und Petrographische Mitteilungen* **53**, 355–78.
- CONNOLLY, J. A. D. 1990. Multivariable phase diagrams: an algorithm based on generalized thermodynamics. *American Journal of Science* **290**, 666–718.
- CORTESOGNO, L. & FORCELLA, F. 1978. Il Massiccio cristallino di Arenzano, frammento di crosta continentale Brianzonese al margine meridionale del Gruppo di Voltri. *Rendiconti della Società Geologica Italiana* **28**, 225–7.
- CORTESOGNO, L., FORCELLA, F., LUCCHETTI, G. & ROSSI, P. M. 1981. Paragenesi di alta pressione e bassa temperatura in un klippe di metaofioliti nel settore nord-occidentale del Massiccio di Voltri. *Rendiconti Società Italiana di Mineralogia e Petrologia* **37**, 447–80.
- CORTESOGNO, L., GALBIATI, B. & PRINCIPI, G. 1980. Le breccie serpentinitiche giurassiche della Liguria orientale. *Archives des Sciences Genève* **33**, 185–200.
- CORTESOGNO, L., GALBIATI, B. & PRINCIPI, G. 1981. Descrizione dettagliata di alcuni caratteristici affioramenti di breccie serpentinitiche della Liguria orientale ed interpretazione in chiave geodinamica. *Ophioliti* **6**, 47–76.
- CORTESOGNO, L., LUCCHETTI, G. & MASSA, B. 1981. Rocce oficarbonate e marmi a silicati nel Massiccio di Voltri: origine e significato, chimismo dei minerali ed equilibri paragenetici. *Rendiconti Società Italiana di Mineralogia e Petrologia* **37**, 481–507.
- DAVIS, P. B. & WHITNEY, D. L. 2006. Petrogenesis of lawsonite and epidote eclogite and blueschist, Sivrihisar Massif, Turkey. *Journal of Metamorphic Geology* **24**, 823–49.
- FEDERICO, L., CAPPONI, G., CRISPINI, L. & SCAMBELLURI, M. 2004. Exhumation of alpine high-pressure rocks: insights from petrology of eclogite clasts in the Tertiary Piedmontese basin (Ligurian Alps, Italy). *Lithos* **74**, 21–40.
- FEDERICO, L., CAPPONI, G., CRISPINI, L., SCAMBELLURI, M. & VILLA, M. I. 2005. $^{39}\text{Ar}/^{40}\text{Ar}$ dating of high-pressure rocks from the Ligurian Alps: evidence for a continuous subduction–exhumation cycle. *Earth and Planetary Science Letters* **240**, 668–80.
- FEDERICO, L., CRISPINI, L., SCAMBELLURI, M. & CAPPONI, G. 2007a. Ophiolite mélange zone records exhumation in a fossil subduction channel. *Geology* **35**, 499–502.
- FEDERICO, L., CRISPINI, L., SCAMBELLURI, M. & CAPPONI, G. 2007b. Different PT paths recorded in a tectonic mélange (Voltri Massif, NW Italy): implications for the exhumation of HP rocks. *Geodinamica Acta* **20**, 3–19.

- FORNERIS, J. F. & HOLLOWAY, J. R. 2004. Evolution of mineral compositions during eclogitization of subducting basaltic crust. *American Mineralogist* **89**, 1516–24.
- GHENT, E. D., STOUT, M. Z. & ERDMER, P. 1993. Pressure-temperature evolution of lawsonite-bearing eclogites, Pinchi Lake, British Columbia. *Journal of Metamorphic Geology* **11**, 279–90.
- GHENT, E. D., TINKHAN, D. & MARR, R. 2009. Lawsonite eclogites from the Pinchi Lake area, British Columbia – new P-T estimates and interpretation. *Lithos* **109**, 248–53.
- GROppo, C., ROLFO, F., SACHAN, H. K. & RAI, S. K. 2016. Petrology of blueschist from the Western Himalaya (Ladakh, NW India): exploring the complex behavior of a lawsonite-bearing system in a paleo-accretionary setting. *Lithos* **252**, 41–56.
- HANSEN, L. D., DIPPLE, G. M., GORDON, T. M. & KELLET, D. W. A. 2005. Carbonated serpentinite (listwanite) at Atlin, British Columbia: a geological analogue to carbon dioxide sequestration. *The Canadian Mineralogist* **43**, 225–39.
- HARLOW, G. E., HEMMING, S. R., LALLEMANT, H. G., SISSON, V. B. & SORESEN, S. S. 2004. Two high-pressure low-temperature serpentinite-matrix melange belts, Motagua Fault zone, Guatemala: a record of Aptian and Maastrichtian collisions. *Geology* **32**, 17–20.
- HOLLAND, T., BAKER, J. & POWELL, R. 1998. Mixing properties and activity-composition relationships of chlorites in the system MgO-FeO-Al₂O₃-SiO₂-H₂O. *European Journal of Mineralogy* **10**, 395–406.
- HOLLAND, T. & POWELL, R. 1996. Thermodynamics of order-disorder in minerals. Symmetric formalism applied to solid solutions. *American Mineralogist* **81**, 1425–37.
- HOLLAND, T. & POWELL, R. 1998. An internally consistent thermodynamic data set for phases of petrological interest. *Journal of Metamorphic Geology* **16**, 309–43.
- KELEMEN, P. B. & MANNING, C. E. 2015. Reevaluating carbon fluxes in subduction zones, what goes down, mostly comes up. *PNAS* **112**, E3997–E4006.
- KERRICK, D. M. & CONNOLLY, J. A. D. 1998. Subduction of ophiicarbonates and recycling of CO₂ and H₂O. *Geology* **26**, 375–8.
- KRETZ, R. 1983. Symbols for rock-forming minerals. *American Mineralogist* **68**, 277–9.
- KROGH, E. J. 1982. Metamorphic evolution of Norwegian country-rock eclogites, as deduced from mineral inclusions and compositional zoning in garnets. *Lithos* **15**, 305–21.
- HAWTHORNE, F. C., OBERTI, R., HARLOW, G. E., MARESCH, W. V., MARTIN, R. F., SCHUMACHER, J. C. & WELCH, M. D. 2012. IMA Report. Nomenclature of the amphibole supergroup. *American Mineralogist* **97**, 2031–48.
- LARDEAUX, J.-M., CARON, J.-M., NISIO, P., PÉQUIGNOT, G. & BOUDEULLE, M. 1986. Microstructural criteria for reliable thermometry in low-temperature eclogites. *Lithos* **19**, 187–203.
- LIU, J. G., ZHANG, R., ERNST, W. G., LIU, J. & MCLIMANS, R. 1998. Mineral parageneses in the Piampaludo eclogitic body, Gruppo di Voltri, Western Ligurian Alps. *Schweizerische Mineralogische und Petrographische Mitteilungen* **78**, 317–35.
- LÓPEZ-CARMONA, A., ABATI, J., PITRA, P. & LEE, J. K. W. 2014. Retrogressed lawsonite blueschists from the NW Iberian Massif: P–T–t constraints from thermodynamic modelling and ⁴⁰Ar/³⁹Ar geochronology. *Contributions to Mineralogy and Petrology* **167**, 987.
- LÓPEZ-CARMONA, A., KUSKY, T. M., SANTHOS, M. & ABATI, J. 2011. P-T and structural constraints of lawsonite and epidote blueschists from Liberty Creek and Seldovia: tectonic implications for early stages of subduction along the southern Alaska convergent margin. *Lithos* **121**, 100–16.
- LÓPEZ-CARMONA, A., PITRA, P. & ABATI, J. 2013. Blueschist-facies metapelites from the Malpica–Tui Unit (NW Iberian Massif): phase equilibria modelling and H₂O and Fe₂O₃ influence in high-pressure assemblages. *Journal of Metamorphic Geology* **31**, 263–80.
- MALATESTA, C., CRISPINI, L., FEDERICO, L., CAPPONI, G. & SCAMBELLURI, M. 2012a. The exhumation of high pressure ophiolites (Voltri Massif, Western Alps): insights from structural and petrologic data on meta-gabbro bodies. *Tectonophysics* **568/569**, 102–23.
- MALATESTA, C., GERYA, T., SCAMBELLURI, M., FEDERICO, L., CRISPINI, L. & CAPPONI, G. 2012b. Intraoceanic subduction of “heterogeneous” oceanic lithosphere in narrow basins: 2D numerical modeling. *Lithos* **140–141**, 234–51.
- MARUYAMA, S., ISOZAKI, Y., KIMURA, G. & TERABAYASHI, M. 1997. Paleogeographic maps of the Japanese Islands: plate tectonic synthesis from 750 Ma to the present. *Island Arc* **6**, 121–42.
- MATTINSON, C. G., ZHANG, R. Y., TSUJIMORI, T. & LIU, J. G. 2004. Epidote-rich talc-kyanite-phengite eclogites, Sulu terrane, eastern China: P-T-f(O₂) estimates and the significance of the epidote-talc assemblage in eclogite. *American Mineralogist* **89**, 1772–83.
- MCBIRNEY, A., AOKI, K. I. & BASS, M. N. 1967. Eclogites and jadeite from Motagua Fault Zone Guatemala. *American Mineralogist* **52**, 908–18.
- MORIMOTO, N., FABRIES, J., FERGUSON, A. K., GINZBURG, I. V., ROSS, M., SEIFERT, F. A., ZUSSMAN, J., AOKI, K. & GOTTARDI, G. 1988. Nomenclature of pyroxenes. *American Mineralogist* **73**, 1123–33.
- OCH, D. J., LEITCH, E. C., CAPRARELLI, G. & WATANABE, T. 2003. Blueschist and eclogite in a tectonic melange, Port Macquarie, New South Wales, Australia. *Mineralogical Magazine* **67**, 609–24.
- OH, C. W., LIU, J. G. & MARUYAMA, S. 1991. Low-temperature eclogites and eclogitic schist in Mn-rich metabasites in Ward Creek, California – Mn and Fe effects on transition between blueschist and eclogite. *Journal of Petrology* **32**, 275–302.
- OKAMOTO, K. & MARUYAMA, S. 1999. The high-pressure synthesis of lawsonite in the MORB + H₂O system. *American Mineralogist* **84**, 362–73.
- PARKINSON, C. D., MIYAZAKI, K., WAKITA, K., BARBER, A. J. & CARSWELL, D. A. 1998. An overview and tectonic synthesis of the pre-Tertiary very-high pressure metamorphic and associated rocks of Java, Sulawesi and Kalimantan, Indonesia. *Island Arc* **7**, 184–200.
- POLI, S. & SCHMIDT, M. W. 1995. H₂O transport and release in subduction zones: experimental constraints on basaltic and andesitic systems. *Journal of Geophysical Research: Solid Earth* **100**, 22299–314.
- POLI, S. & SCHMIDT, M. W. 1997. The high-pressure stability of hydrous phases in orogenic belts: an experimental approach on eclogite-forming processes. *Tectonophysics* **273**, 169–84.
- RAMSAY, J. G. & HUBER, M. I. 1987. *The Techniques of Modern Structural Geology. Vol. 2: Folds and Fractures*. London: Academic Press, 700 pp.
- RAVNA, E. J. K., ANDERSEN, T. B., JOLIVET, L. & DE CAPITANI, C. 2010. Cold subduction and the formation of lawsonite eclogite – constraints from prograde

- evolution of eclogitized pillow lava from Corsica. *Journal of Metamorphic Geology* **28**, 381–5.
- RUBATTO, D. & SCAMBELLURI, M. 2003. U–Pb dating of magmatic zircon and metamorphic baddeleyite in the Ligurian eclogites (Voltri Massif, Western Alps). *Contributions to Mineralogy and Petrology* **146**, 341–55.
- SCAMBELLURI, M., BEBOUT, G. E., BELMONTE, D., GILIO, M., CAMPOMENOSI, N., COLLINS, N. & CRISPINI, L. 2016. Carbonation of subduction-zone serpentinite (high-pressure ophiocarbonate; Ligurian Western Alps) and implications for the deep carbon cycling. *Earth and Planetary Science Letters* **441**, 155–66.
- SCAMBELLURI, M., HOOGERDUIN STRATING, E. H., PICCARDO, G. B., VISSERS, R. L. M. & RAMPONE, E. 1991. Alpine olivine and titanite clinohumite bearing assemblages in the Erro–Tobbio peridotites. *Journal of Metamorphic Geology* **9**, 79–91.
- SCHMIDT, M. W. & POLI, S. 1998. Experimentally based water budgets for dehydrating slabs and consequences for arc magma generation. *Earth and Planetary Science Letters* **163**, 361–79.
- SHIBAKUSA, H. & MAEKAWA, H. 1997. Lawsonite-bearing eclogitic metabasites in Cazadero area, northern California. *Mineralogy and Petrology* **61**, 163–80.
- SPANDLER, C. & PIRARD, C. 2013. Element recycling from subducting slabs to arc crust: a review. *Lithos* **170–171**, 208–23.
- TSUJIMORI, T. & ERNST, W. G. 2014. Lawsonite blueschists and lawsonite eclogites as proxies for palaeo-subduction zone processes: a review. *Journal of Metamorphic Geology* **32**, 437–54.
- TSUJIMORI, T., LIU, J. G. & COLEMAN, R. G. 2005. Co-existing retrograde jadeite and omphacite in a jadeite-bearing lawsonite eclogite from the Motagua Fault Zone, Guatemala. *American Mineralogist* **90**, 836–42.
- TSUJIMORI, T., SISSON, V. B., LIU, J. G., HARLOW, G. E. & SORENSEN, S. S. 2006a. Very-low-temperature record of the subduction process: a review of worldwide lawsonite eclogites. *Lithos* **92**, 609–24.
- TSUJIMORI, T., SISSON, V. B., LIU, J. G., HARLOW, G. E. & SORENSEN, S. S. 2006b. Petrologic characterization of Guatemalan lawsonite eclogite: eclogitization of subducted oceanic crust in a cold subduction zone. In *Ultra-high-Pressure Metamorphism: Deep Continental Subduction* (eds B. H. Hacker, W. C. McClelland & J. G. Liou), pp. 147–68. Geological Society of America Special Papers no. 403.
- USUI, T., NAKAMURA, E. & HELMSTAED, H. 2006. Petrology and geochemistry of eclogite xenoliths from the Colorado Plateau: implications for the evolution of subducted oceanic crust. *Journal of Petrology* **47**, 929–64.
- USUI, T., NAKAMURA, E., KOBAYASHI, K. & MARUYAMA, S. 2003. Fate of the subducted Farallon plate inferred from eclogite xenoliths in the Colorado Plateau. *Geology* **31**, 589–92.
- VIDAL, O. & PARRA, T. 2000. Exhumation paths of high-pressure metapelites obtained from local equilibria for chlorite-phengite assemblages. *Geological Journal* **35**, 139–61.
- VIGNAROLI, G., ROSSETTI, F., BOUYBAOUENE, M., MASSONNE, H. J., THEYE, T., FACCENNA, C. & FUNICIELLO, R. 2005. A counter-clockwise P–T path for the Voltri Massif eclogites (Ligurian Alps, Italy). *Journal of Metamorphic Geology* **23**, 533–55.
- VITALE BROVARONE, A. & BEYSSAC, O. 2014. Lawsonite metasomatism: a new route for water to the deep Earth. *Earth and Planetary Science Letters* **393**, 275–84.
- VITALE BROVARONE, A., GROppo, C., HETÉNYI, G., COMPAGNONI, R. & MALAVIEILLE, J. 2011. Coexistence of lawsonite-bearing eclogite and blueschist: phase equilibria modelling of Alpine Corsica metabasalts and petrological evolution of subducting slabs. *Journal of Metamorphic Geology* **29**, 583–600.
- WATSON, K. D. & MORTON, D. M. 1969. Eclogite inclusions in kimberlite pipes at Garnet Ridge, northeastern Arizona. *American Mineralogist* **54**, 267–85.
- WEI, C. J. & POWELL, R. 2003. Phase relations in high-pressure metapelites in the system KFMASH (K₂O–FeO–MgO–Al₂O₃–SiO₂–H₂O) with application to natural rocks. *Contributions to Mineralogy and Petrology* **145**, 301–15.
- WHITE, R. W., POWELL, R. & PHILLIPS, G. N. 2003. A mineral equilibria study of the hydrothermal alteration in mafic greenschist facies rocks at Kalgoolie, Western Australia. *Journal of Metamorphic Geology* **21**, 455–68.
- WHITNEY, D. L. & EVANS, B. W. 2010. Abbreviations for names of rock-forming minerals. *American Mineralogist* **95**, 185–7.
- ZACK, T., RIVERS, T., BRUMM, R. & KRONZ, A. 2004. Cold subduction of oceanic crust: implications from a lawsonite eclogite from the Dominican Republic. *European Journal of Mineralogy* **16**, 909–16.
- ZHANG, J. X. & MENG, F. C. 2006. Lawsonite-bearing eclogites in the north Qilian and north Altyn Tagh: evidence for cold subduction of oceanic crust. *Chinese Science Bulletin* **51**, 1238–44.
- ZHANG, J. X., MENG, F. C. & WAN, Y. S. 2007. A cold Early Paleozoic subduction zone in the North Qilian Mountains, NW China: petrological and U–Pb geochronological constraints. *Journal of Metamorphic Geology* **25**, 285–304.
- ZUCALI, M. & SPALLA, M. I. 2011. Prograde lawsonite during the flow of continental crust in the Alpine subduction: strain vs. metamorphism partitioning, a field-analysis approach to infer tectonometamorphic evolutions (Sesia-Lanzo Zone, Western Italian Alps). *Journal of Structural Geology* **33**, 381–98.